ALGORITHM FOR IMPROVING THE DETERMINATION OF TERRIGENOUS ROCK PERMEABILITY

Vaqif Seidov, Khalid Melikov, Afet Samadzadeh

Azerbaijan State Oil and Industry University
vagif1439@gmail.com
xalid_melikov@yahoo.com
afasamedzade392@gmail.com

Abstract

This paper analyses the current methods used to determine the permeability of rocks, as well as the challenges involved in this process. An improved methodology was developed for determining the permeability of terrigenous rocks using petrophysical, well geophysical and direct methods. The paper provides an overview of how the methodology is implemented and applied. This methodology can be summarized as follows: - The coefficients of variation of permeability obtained by well geophysical survey methods, hydrodynamic logging and rock sampling are compared. - A graphical dependence is created between oil-water phase permeability and water saturation, as well as between oil-water phase permeability and effective permeability. - A graph is created to compare the coefficient of specific productivity with the coefficient of average effective permeability. The oil or water saturation of the formations is analyzed according to the situation of the points characterizing the wells. Significant differences in permeability values are observed based on data from hydrodynamic logging, rock sampling, and well geophysical survey methods. The low permeability value is due to relative permeability in productive and water-bearing layers. Effective permeability does not permit the formation of a layer filtration model. Therefore, it is advisable to conduct research using hydrodynamic logging in 20 cm steps. In this case, the margin of error in the determined effective permeability decreases. There is also a close correlation between the coefficient of specific productivity and effective permeability. To increase the accuracy of the results, all three studies must be conducted together. This methodology can be applied to any oil or gas field.

Keywords: permeability, phase permeability, hydrodynamic logging, well geophysical survey, rock sample, packing

I. Introduction

Rocks consist of a mineral skeleton, or solid phase, and a pore space usually filled with liquid and gas components.

Permeability is the property of rocks to transmit liquids, gases and their mixtures in the presence of a pressure gradient. Permeability is a parameter characterizing the ability of reservoir rocks to transmit fluid.

Absolute permeability is the permeability of a rock in the case of filtration through it of a homogeneous liquid or gas inert with respect to the surface of the solid phase. Phase permeability is the ability of rocks saturated with a mixture of oil, gas and water or any other inhomogeneous fluid to permeate its individual phases.

Relative permeability of a porous medium is the ratio of phase permeability of this medium for a given phase to absolute permeability. To estimate the permeability of rocks, the linear Darcy filtration law is usually used. According to the values of permeability coefficient, rocks are divided into permeable (gravels, sands, weakly cemented sandy-clay sediments, cavernous carbonate sediments), semi-permeable (clayey sands, finely fractured chalky limestones and dolomites) and

practically impermeable (clays, argillites, shales, marls, densely cemented sandstones and siltstones, dense chalk and limestone).

The permeability of the rocks is based on the difference in the pressures created in the reservoirs' pores, and the rock's ability to release the fluids filling the pores is assumed. The studied quantity is characteristically a dynamic quantity, characterizing the fluid's displacement in the rock's pores. Permeability is considered the most dynamic quantity in reservoir rocks. Therefore, the limit of change of permeability does not correspond to the value of the rock's porosity in most cases. It is difficult to explain logically [1,7,10,11]. Predicting the correlation of its relationship with other static quantities (clayness, sandiness, etc.) often does not allow the estimation of permeability [8,9,14]. This complicates the interpretation of geophysical data and the study of rock samples in the laboratory. The relationships obtained do not sufficiently reflect the properties of reservoir rocks, which are observed in all wells located in the Bahar field. As a result, the error that can be omitted in the operative interpretation obtained based on the data of well geophysical survey (WGS) methods increases [2,3,13]. To increase the accuracy of the results obtained, it is necessary to use the data of hydrodynamic logging (HDL - direct method), WGS, and rock samples jointly.

II. Exploration target

The sections of oil and gas wells located in Azerbaijan are mainly represented by terrigenous rocks. The Bahar oil and gas condensate field is located in the Caspian Sea, 40 km south-east of Baku and 20 km south of Qum Island (Fig.1).

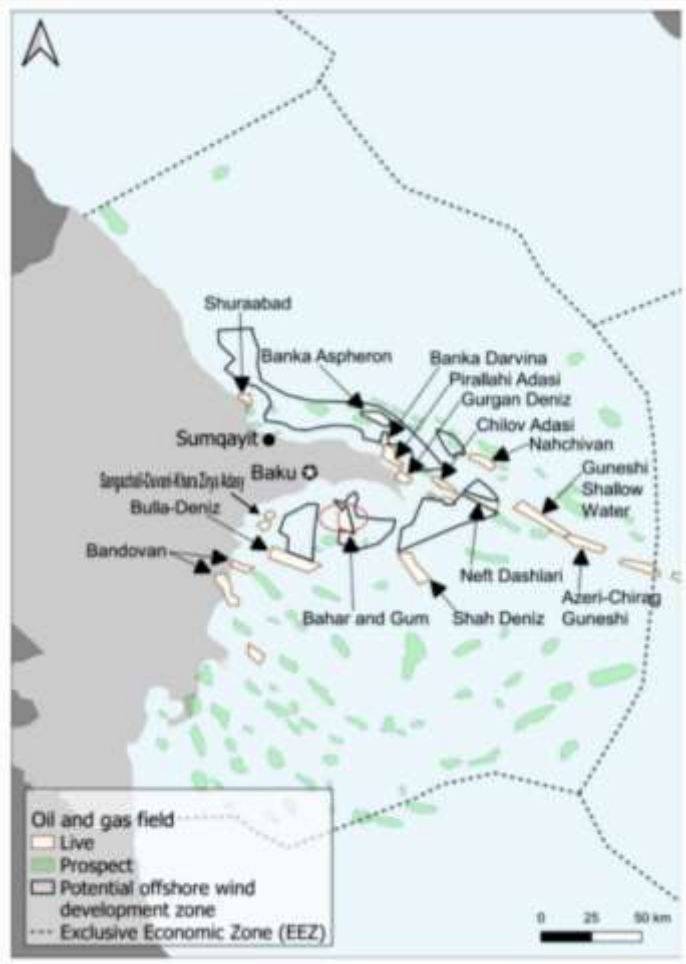

Figure 1: *Schematic map of oil and gas fields in Azerbaijan.*

The upper Miocene–Quaternary sedimentary complex is present in the part of the Bahar field section that has been drilled. The geological section includes deposits from the Miocene, Productive Series, Akchagyl stage and Quaternary period.The Productive Series consists of lower and upper parts and is subdivided into suites and horizons: Sub-Kirmaky (SK), Kirmaky, Upper Kirmaky Sandy (UKS), Upper Kirmaky Caleyey (UKC), Fasila, as well as the Balakhany (horizons V, VI, VII, VIII, IX, X), Sabunchi (horizons I, III, IV, IVa, IVb) and Surakhany (horizon I) reservoir suites. The Fasila Suite the upper part of the Productive Series has the highest sand content — 73%, of which 10% is sandstone.

The structure is complicated by regional and local tectonic disturbances and divided into eight tectonic blocks. The Bahar structure extends in a north-south direction. However, near the southern periclinal, this extension turns to the south-east. The northern periclinal of the structure is elongated, while the southern one is shorter. The saddle of the structure is located in its southern part, near a mud volcano that complicates the southern slope. Among the eight tectonic blocks of the deposit, blocks I, II and III are considered to be the main ones in terms of hydrocarbon content.

In Blocks II and III, the Fasila Suite forms oil and gas condensate fields, with hydrocarbon flows generally being mixed in nature. In these reservoir layers, oil (with a gas cap) was first discovered on the western wing of the anticline in Block III, and on the eastern wing with the presence of gas condensate also being detected. Gas inflows were obtained in Block III, and the presence of oil is considered likely [5].

III. Methodology

Research with HDL in the well is carried out in the following stages: packaging in the research area; creating hydrodynamic excitation of the layer; closing the packer.

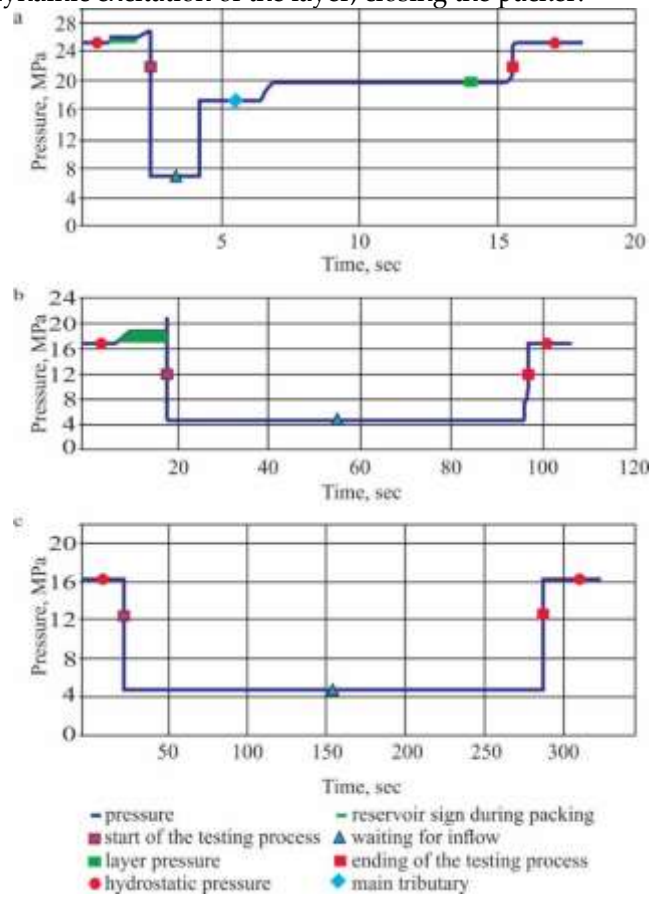

Figure 2: *An example of a hydrodynamic logging pressure diagram*

Hydrodynamic logging refers to direct methods of investigation. With this method the formation pressure is recorded in graphical form (Fig. 2 a, b, c). The graph, as a rule, is divided into three parts:

1) At the first stage, the logging device is installed with the packer and put into operation (differential pressure is created); high pressure is recorded for a certain time (left part of the graphs);
2) After the fluid withdrawal process begins, the graph shows a rapid decrease in pressure.
3) When fluid begins to move out of the reservoir, the pressure curve stabilizes, reflecting the actual reservoir pressure.

During the survey, fluid flows from the reservoir into a special section on the logging tool and the water or oil content is determined from the sample.

When applying hydrodynamic logging in a well, the primary measured quantity is layer pressure (fig. 2).

A sharp increase in the graph during packing indicates the presence of mud cake, and this feature belongs to reservoir layers (Fig. 2a). After a sharp rise, the pressure decreases sharply, which indicates the awakening of the layer. In the other two cases, no growth is noted in the graph during packing.

In the first case (Fig. 2b) 20-100 seconds, and in the second case (Fig. 2c) 20-300 seconds, the flow through the layer is not recorded, during this period, there is no change in the graph of pressure. This shows that the permeability is different for the thickness of the layers.

Filtrate movement in the reservoir depends directly proportional to the effective porosity of rocks and inversely proportional to its viscosity. Therefore, the mobility of the filtrate in front of each depressed layer is calculated by the following formula [4,6,12]:

$$\frac{k_{ef}}{\mu} = \frac{V_i}{A\Delta t_i \Delta P_i} \quad (1)$$

where A is the coefficient that considers the geometry (flowability) of the fluid entering the well from the rock; V_i is the volume of the filtrate causing the depression; Δt_i is the time the filtrate percolates through the layer; ΔP_i is the pressure difference during the depression; an average value of effective permeability coefficient k_{ef}, μ is the viscosity of the filtrate.

The research is carried out in the following order:

- rock sampling: - determination of oil saturation (S_{oil}), porosity coefficient (k_p), an average value of effective permeability coefficient (k_{ef}), and coefficient of variation of permeability (W_k) in small-grained and low-clay rocks;
- study of WGS data: layer thickness (h), porosity coefficient (k_p), probable permeability (k_{per}), coefficient of variation of permeability (W_k);
- investigation of hydrodynamic logging data: the thickness (h_{HDL}), the average value of the effective permeability coefficient (k_{ef}) and coefficient of variation of permeability (W_k) of the studied interval.

After determining these data, the coefficients of permeability variation obtained by WGS, HDL, and rock sampling are compared.

The graph is based on geophysical logging data between the permeability of the oil-water phase (considering the absolute gas permeability (k_{oil}+k_w)/k_g) and the water saturation (Sw) is the percentage value of water).

The graph is analyzed: the reference value of k_{ef} in the washout zone is taken, and the permeability prediction under current oil saturation conditions is given. For this purpose, a relative value characterizing the relationship between water-oil saturation and effective porosity is determined using the following relationship:

$$\frac{(k_{oil}+k_w)/k_g}{k_{ef}/k_g} = \frac{k_{oil}+k_w}{k_{ef}} = a; \;\; k_{oil} + k_w = ak_{ef} \quad (2)$$

where,

k_{oil} is the permeability of the oil phase;

k_w is the permeability of the water phase; a is the value characterizing the ratio of water-oil saturation and effective porosity coefficient;
k_g is the absolute gas permeability coefficient.

A comparison graph between the specific productivity coefficient (k_{core}/k_{HDL}) and the average effective permeability coefficient (k_{ef}) is constructed and analyzed.

Application. As indicated in the methodology, the WGS – Neutron methods, rock sample – 56 and HDL data of 4 intervals on the rocks that comprise the studied formation (Fasila Suite) for Bahar field were collected and analyzed for the 4 wells. For the application of the methodology, information was collected on conventional wells A, B, C, and D, and a graph was made between the permeability of the water-oil phase [(k_{oil}+k_w)/k_g] and the water saturation (S_w) (Fig. 3).

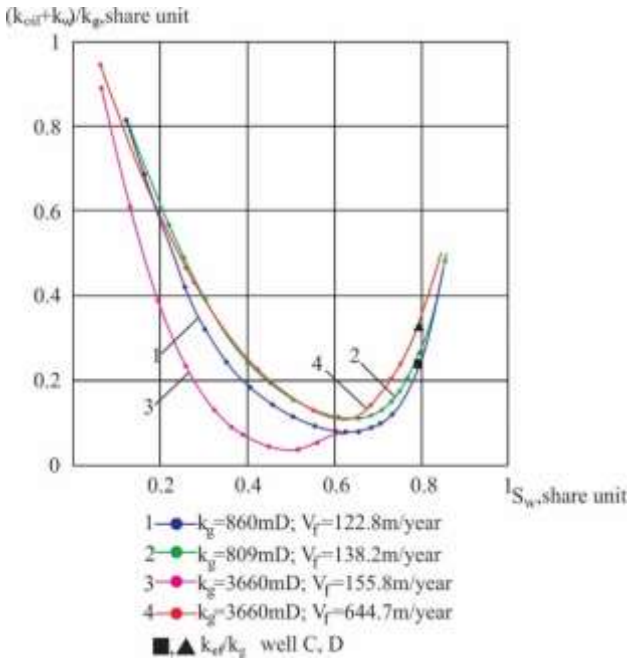

Figure 3: *Graph of the relationship between water-oil phase permeability and water saturation. (1) k_g=860 mD, V_f=12.8 m/year (annual change in water saturation according to field operation data); (2) k_g =809 mD, V_f=238.2 m/year; (3) k_g =3660 mD, V_f=155.8 m/year; (4) k_g =3660 mD, V_f=644.7 m/year.*

k_g is the absolute gas permeability coefficient; V_f is the filtrate rate; k_{ef} is the effective permeability.

As can be seen in the figure, in wells C and D, the relationship between (k_{oil}+k_w)/k_g and S_w coincides up to S_w = 0.65. After this point, the dependencies begin to diverge. In order to evaluate this section, a computational processing was carried out.

An estimate of the k_{ef}/k_g ratio for well D based on data from well C is presented in the following Table 1, where we replace $\frac{(k_{oil}+k_w)/k_g}{k_{ef}/k_g}$ with W for well D:

Table 1: *Estimation of k_{ef}/k_g for Well D Using W Parameter*

For well C					For well D
Water saturation, %	Oil saturation, %	(k_{oil}+k_w)/k_g	k_{ef}/k_g	W	k_{oil}+k_w=k_{ef}·W
20	80	0,62	0,242	2,256	0,59
50	50	1,12-0,16	0,242	0,58	0,13
40-30	60-70	0,32-0,38	0,242	1,037	0,24

Under these conditions, the report's results for well D will be the same as the results of borehole C. This is because the lithological composition and conditions of the studied interval are the same. So, since the comparison is used in our methodology, rocks of the same composition and age belonging to the same layer suite in different wells are taken as the research object.

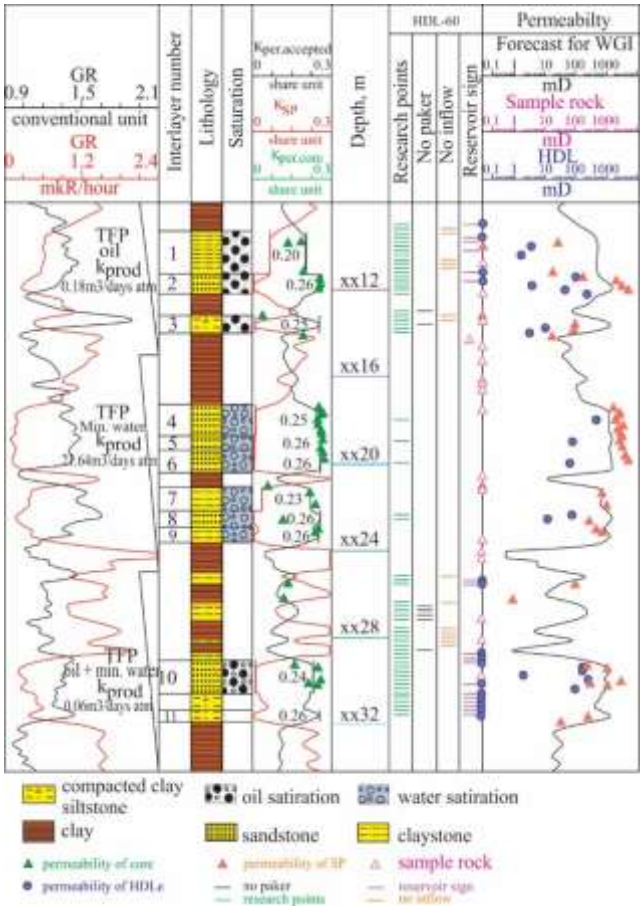

Figure 4: *Logging curves and results obtained in the well B*

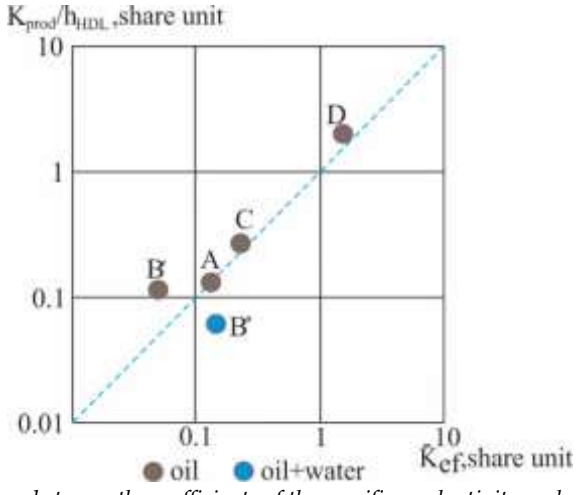

Figure 5: *Comparison between the coefficients of the specific productivity and effective permeability*

This calculation for 4 wells shows that when S_{oil}=80%, the permeability of the oil-water phase (k_{oil}+k_w) is 2-3 times larger (0.62>0.23), and when S_{oil}=40-50% it is 1.7 times smaller (0.14<0.23). When S_{oil}=60-70%, the permeability of the oil-water phase corresponds to k_{ef} (0.23851=0.24), it is

approximately equal (These results are derived from the comparative analysis carried out in the corresponding report). The results obtained in wells A and B are slightly different, and the reason for this is given below (Fig.5). Logging curves in borehole B are provided as an example (Fig. 4).

Analyzing the build graph, it appears that three features are obtained. The position of the points characterizing the wells is different compared to the trend line:

- lies in a straight trend line (A, C, D) – the resulting product is a mixture of water and oil;
- below the trend line ($B^{//}$) – dominated by water;
- above the trend line ($B^{/}$) - dominated by oil.

Point $B^{/}$ is associated with high filtration recorded in formations №1, 2 and 3. At the same time, according to the results of HDL, point $B^{//}$ is explained by watering of formations №10 and 11. Thus, based on the adjusted graph, the saturation of the studied formations in the wells is determined unambiguously.

A comparison graph was build for 4 wells of selected filed between the coefficient of specific productivity (k_{prod}/h_{HDL}) and the effective permeability (k_{ef}) (Fig. 5).

IV. Conclusion

- The obtained results show a sharp difference in the values of permeability obtained based on HDL, rock sample, and WGS data (depends on geologic conditions);
- The permeability values determined by hydrodynamic logging (HDL) are underestimated compared to other methods in oil-saturated and watered reservoirs;
- It is impossible to build a full-fledged reservoir filtration model based on effective permeability based on HDL data alone;
- It is reasonable to perform hydrodynamic logging with a uniform step of 20 cm for the studied wells. In this case, the magnitude of the error in certain effective permeability tends to decrease, which is due to the lithologic composition of rocks in the section of this well;
- We see that there is a close correlation between the specific productivity coefficient and the effective permeability (however, this relationship decreases as the clay content of the rocks increases);
- Conducting all three studies together increases the accuracy of the obtained results (in the absence of at least one of them, the degree of reliability is significantly reduced).

CONFLICT OF INTEREST.

Authors declare that they do not have any conflict of interest.

References

[1] Akhmedov, T.R., Aghayeva, M.A. Prediction of petrophysical characteristics of deposits in Kurovdagh field by use of attribute analysis of 3D data. // *Geofizicheskiy Zhurnal*, 2022. Vol. 44, No 3, 103-112, DOI: https://doi.org/10.24028/gj.v44i3.261976.

[2] Bloomfield, J.P., Williams, A.T. An empirical liquid permeability – gas permeability correlation for use in aquifer properties studies. // *Journal of Engineering Geology & Hydrogeology*, 1995. Vol. 28 (Supplement 2), pp. S143-S150, https://doi.org/10.1144/GSL.QJEGH.1995.028.S2.05 .

[3] Fischer, G., Paterson, M.Chapter Measurement of permeability and storage capacity in rocks during deformation at high temperature and pressure. // *Int. Geophysics*, 1992. Vol. 51, pp. 213-252.

[4] Heller, R., Vermylen, J., Zoback M. Experimental investigation of matrix permeability of gas shales. // *AAPG Bull.*, 2014. Vol. 98, pp. 975-995.

[5] Ismailov F., Salmanov A., Maharramov B., Shakarov H.. Oil and gas fields and promising structures of Azerbaijan. Caspian Sea waters (Reference book). Baku: MSV MMC Publishing House. 2024. 648 p. (in Azerbaijani).

[6] Jinlong,F., Hywel,R.Th., Chenfeng, L. Tortuosity of porous media: Image analysis and physical simulation. // *Earth-Science Reviews*, 2021. Vol.212, pp. 103439, DOI: 10.1016/j.earscirev.2020.103439.

[7] Kerimova, K.A., Aliyev, N.E. Study of the interrelation between the geneses and reservoir properties of productive series deposits in Pirallahi field on the basis of oil-field geophysical data. // *Geofizicheskiy Zhurnal*, 2022.Vol. 44, No 4,pp. 146-154, DOI: https://doi.org/10.24028/gj.v44i4.264849

[8] Oshnyakov, I.O., Xabarov, A.V., Mitrofanov, D.A., Loznyuk, O.AThe study of the deposits of the Berezovsky suite according to the data of the extended well logging complex and core studies on the example of the Kharampur field. // *STN "Karotajnik"*, Tver: Pub. AIS.Rel.6 (300), 2019. pp.103-117. (in Russian).

[9] Parubenko, I.V., Alekseyeva, D.I., Akimova, O.A., Xabarov, A.V. Analysis of an extended set of well logging and core studies to identify complex low-permeability reservoirs. // *STN "Karotajnik"*, Tver: Pub. AIS.Rel.6(300), 2019. pp.118-133. (in Russian).

[10] Reading: Porosity and Permeability. Geology. courses.lumenlearning.com. Retrieved. 2022. 01-14.

[11] Seidov, V.M., Khalilova, L.N. Examples of reconstruction of productive strata depositional environment in Azerbaijan on the base of well logging data. // *Neftyanoe Khozyaystvo (Oil Industry)*, 2019, Issue 05, pp.62-66, https://doi.org/10.24887/0028-2448-2019-5-62-66 (in Russian).

[12] Sigal, R.F. The pressure dependence of permeability. // *Petrophysics – SPWLA J. Form. Eval. Reserv. Descr.*, 2002. Vol. 43, pp. 92-02.

[13] Sowinski, D. et al. Poroelasticity as a model of soft tissue structure: hydraulic permeability reconstruction for magnetic resonance elastography in silico". // *Frontiers in Physics*, 2021. Vol.8, 617582. doi: 10.3389/fphy.2020.617582.

[14] Zubik, A.O., Shumatbayev, K.D., Privalova, O.P., Amineva, Q.R. Analysis of the results of using typified petrophysical reservoir models in assessing the geological reserves of oil in the fields of the Republic of Bashkortostan. // *STN "Karotajnik"*, Tver: Pub. AIS. Rel.6(300), 2019. pp.144-159. (in Russian).